Journal of Sustainable Construction Materials and Technologies
Web page info: https://jscmt.yildiz.edu.tr
DOI: 10.47481/jscmt.1142100

JSCMT
Journal of Sustainable Construction Materials and Technologies

Research Article

Natural pozzolan–based green geopolymer foam for thermal insulation

Kübra EKİZ BARIŞ*, Leyla TANAÇAN

Department of Architecture, İstanbul Technical University, İstanbul, Türkiye

ARTICLE INFO

Article history
Received: 07 July 2022
Accepted: 18 August 2022

Key words:
Alkali activator, geopolymer foam, natural pozzolan, optical microscopy, porosity, thermal conductivity

ABSTRACT

The current study investigates the possibility of volcanic Tuff of Earth of Datça (ED) in Turkey to be used as an aluminosilicate source in producing a geopolymer foam for thermal insulation. An extensive evaluation of the effects of fine sand–to–pozzolan and Al powder–to–pozzolan ratios on the physical, mechanical, and thermal properties and morphology (porosity, average and maximum pore diameter, pore size distribution) of the pores were carried out. The sodium silicate and potassium hydroxide (12.5 M) solutions with an activator ratio of 2.5 were used as alkali activators, and Al powder was used as a foaming agent. Research results reveal that Earth of Datça is a suitable precursor for producing a geopolymer foam. Fine sand and aluminum powder contents are critical to the optimum foam structure. The addition of finely ground silica sand ensured the volumetric stability of the binder and prevented the collapse after swelling of the binder. The optimum Al powder–to–pozzolan ratio was determined as 0.5% because it gives higher physical, mechanical, and thermal properties due to the more homogenous microstructure with finer pore size and narrower pore size distribution lower degree of interconnectivity between the pores. Research results also show that the natural volcanic Tuff of Datça Peninsula as an aluminosilicate source gives promising results in the field of producing highly porous geopolymers with low thermal conductivity (0.087–0.134 W/mK), high porosity (72.3–82.6%) and an adequate compressive strength (0.40–2.09 MPa). This study contributes to the literature that Earth of Datça–based geopolymer foam may function well as an insulation material for building enclosures.

Cite this article as: Ekiz Barış, & K., Tanaçan, L. (2022). Natural pozzolan–based green geopolymer foam for thermal insulation. *J Sustain Const Mater Technol*, 7(3), 128–144.

1. INTRODUCTION

The building industry is one of the fastest growing industries [1], and buildings are liable for approximately 40% of the total energy consumption [2]. Generally, thermal insulation materials decrease the energy consumption of buildings by decreasing the energy loss. But organic thermal insulation materials are flammable, inorganic thermal insulation materials need complex processing conditions, and high sintering temperature results in higher costs [3] and embodied energy. To reduce the energy consumption and consequently the energy requirement of buildings, apart from using thermal insulation materials, the development of new materials with higher thermal performance is of the utmost importance.

***Corresponding author.**
*E–mail address: ekizk@itu.edu.tr

Published by Yıldız Technical University Press, İstanbul, Türkiye
This is an open access article under the CC BY–NC license (http://creativecommons.org/licenses/by–nc/4.0/).

Cellular or lightweight aggregate concrete materials have been produced to provide energy savings. However, their raw material is Ordinary Portland Cement (OPC), whose production process is energy intensive and emits approximately 1 ton of CO_2 in a ton of production [4]. Recently, geopolymer foams have been produced by creating the gas bubbles into the binder during the chemical reactions between the foaming agent and alkali activator or by incorporating a large volume of readily–prepared air bubbles into the mixture [5], have been produced to replace foamed cementitious materials. Commonly used foaming agents such as finely divided metallic aluminum, hydrogen peroxide, sodium peroxide, sodium perborate, metal silicon, silica fume, and silicon carbide are in the field of promising research [6]. Due to the high volume of pores, they could contribute to the material's thermal performance. Furthermore, they are more sustainable than OPC–based foams since their process emits 0.19–0.24 tonnes of CO_2 in a ton of its production [5], and up to 80% energy savings could be achieved [7].

Up until the present, scores of works have focused on producing highly porous geopolymers (porosity ≥50% or bulk density ≤0.7 g/cm^3 [8]) having low thermal conductivity with different types of aluminosilicate sources. For example, ultrafine perlite–based geopolymer, activated with sodium hydroxide (NaOH) and foamed with hydrogen peroxide (H_2O_2, 0.5–3.0% by weight of aluminosilicate source), exhibits thermal conductivity, porosity, and compressive strength ranging between 0.03–0.06 W/mK, 74–89%, and 0.2–0.8 MPa, respectively [9]. Porous fly ash–based geopolymer was produced using sodium silicate (Na_2SiO_3) as an alkali activator and H_2O_2 (0.05–0.1% by weight of aluminosilicate source) as the foaming agent. The test results reveal that the values of thermal conductivity (0.07–0.09 W/mK), porosity (74–81%), and compressive strength (0.4–1.4 MPa) show promise as thermal insulation material [3]. In another study, biomass fly ash–based–geopolymers were activated by a mixture of NaOH and Na_2SiO_3 and were foamed using H_2O_2 as a pore–forming agent. Foamed geopolymers exhibit thermal conductivity as low as 0.10 W/mK, porosity up to 72.5%, and compressive strength in a range of 1.2–6.6 MPa, depending on the content of the pore–forming agent (0.03–1.20% by weight of aluminosilicate source) [10]. In another research, fly ash–based geopolymer foams were produced by using H_2O_2 or Al powder foaming agents. The specimens containing H_2O_2 have 0.31–0.97 g/cm^3 density and 0.083–0.174 W/mK thermal conductivity, whereas the specimens with Al powder have 0.50–0.77 g/cm^3 density and 0.099–0.159 W/mK thermal conductivity. Study results state that these foams can be used as thermal insulation materials [11]. Fly ash was also foamed with sodium perborate foaming agent in the literature. The study results reveal that the density, thermal conductivity, and compressive strength of geopolymer foams are in the range of 0.64–0.82 g/cm^3, 027–0.32 W/mK, and 4.2–4.8 MPa, respectively [12].

Metakaolin–based geopolymer foam, activated with a mixture of potassium hydroxide (KOH) and potassium silicate (K_2SiO_3) and foamed with silica fume blowing agent, has a thermal conductivity between 0.12 and 0.33 W/mK, and porosity in a range of 65–85% [13]. The characterization of metakaolin–based geopolymer foam contains KOH and K_2SiO_3 as alkali activators and H_2O_2 (5–20%, by weight) as a forming agent, shows that the material with low thermal conductivity (0.11–0.17 W/mK), high porosity (60.2–83.1%), and acceptable compressive strength (0.3–11.6 MPa) could be successfully produced [14]. The pore morphology, density, porosity, thermal conductivity, and compressive strength of metakaolin–based porous geopolymers (containing H_2O_2 chemical pore–forming agent) were researched in another study. These geopolymers have 0.35–1.20 g/cm^3 density, 0.4–5.65 MPa mechanical strength and improved thermal conductivity (0.13–0.32 W/mK) [15]. The influence of the Al powder content (3–12%, by weight) on the properties of the KOH/NaOH+Na_2SiO_3 activated metakaolin–based geopolymer foam was investigated. Material with improved insulating behavior, thermal conductivity of 0.15 W/mK, and porosity of 70% was produced depending on increasing Al powder content [16]. The possibility of using metakaolin–based geopolymer foams foamed with Na_2O_2 to be applied for fire protection was investigated. The foamed material with 0.30–0.46 g/cm^3 density, 0.085–0.115 W/mK thermal conductivity, and 0.6–1.6 MPa compressive strength possess a stable porous structure and excellent fire resistance [17]. The effects of sodium lauryl ether sulfate (SLES) foaming agents on pore types and properties of lightweight kaolinite–based geopolymers were also investigated in the literature. The results show that the lightest geopolymer foam has a porosity of 72.34% and a compressive strength of 4.69 MPa with low thermal conductivity of 0.197 W/mK [18].

Waste glass–based porous geopolymers with thermal conductivity of 0.21 W/mK, porosity of 55%, and compressive strength of 7.3 MPa were produced using a combination of KOH and K_2SiO_3 activators and H_2O_2 (5%, by weight) as pore foaming agent [19]. NaOH–activated bottom ash with varying amounts of Na_2SiO_3 (25–55%, by weight) as the foaming agent has 0.075 W/mK thermal conductivity, 72% porosity, and 3.55 MPa compressive strength and could be used as a thermal insulation material [20]. Waste metakaolin, recycled glass, and steel–plant waste were activated with NaOH+Na_2SiO_3 solutions and foamed with aluminum scrap recycling waste (50% by weight). The results showed that highly porous, lightweight building materials could be obtained with thermal conductivity, porosity, and compressive strength ranging between 0.14–0.15 W/mK, 83–86%, and 1.1–2.0 MPa, respectively [21]. Consequently, geopolymer foams show good insulating properties with thermal

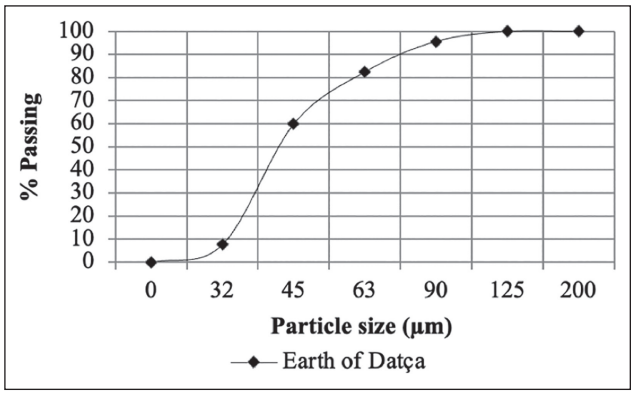


Figure 1. Particle size distribution of volcanic Tuff of Earth of Datça.

conductivities, porosities, and compressive strengths ranging between 0.03–0.33 W/mK, 55–89%, and 0.2–11.6 MPa, respectively, depending on the type and quantity of aluminosilicate source, pore foaming agent, pore foaming agent–to–pozzolan ratio and fine sand–to–pozzolan ratio.

Although much of the research carried out has been based on producing artificial pozzolan–based highly porous geopolymers with improved thermal performance, investigations regarding the production of natural pozzolan–based geopolymer foams are scarce. The natural pozzolan resources of Turkey are at a level that cannot be ignored. Approximately 155.000 km^2 of the country consists of volcanic rocks [22]. Datça pozzolan used in this research is the natural soil of Datça Peninsula. It was formed due to strong volcanic eruptions in Nysiros and Yelli Islands [23].

This research aims to investigate the possibility of volcanic Tuff of Earth of Datça (ED) to be used as an aluminosilicate source in the production of geopolymer foam for thermal insulation. In the scope of the study, key factors such as fine sand–to–pozzolan (FS/P) and Al powder–to–pozzolan (Al/P) ratio affect the physical, mechanical, and thermal characteristics of ED–based geopolymer foam are researched. Optimizing the test results, a new porous material with low thermal conductivity is proposed as an alternative to the existing thermal insulation materials in the building industry.

2. EXPERIMENTAL TECHNIQUES

2.1. Raw Materials

For the production of geopolymer foam, natural Datça pozzolan was used as an aluminosilicate source, and its specific gravity is 2.52 g/cm^3. The specific surface area of the pozzolan, determined using the Blaine method [24], is 5467.75 cm^2/g, and the particle size distribution is shown in Figure 1.

Semi–quantitative element (XRF) and quantitative XRD analysis of the ED and lime–pozzolan mortar (ED)T produced for the pozzolanic activity test were performed in the previous research [22] using Philips 71 PW–2404 XRF and Shimadzu XRD–6000 (Cu X–ray tube 1.5405 Angstrom) equipment, respectively. XRF analysis indicated that (Table 1) Earth of Datça fulfills the requirements of T.S. 25 [25] to be used as a natural pozzolan in cement and other types of binders because its SiO_2+Al_2O_3+Fe_2O_3 content (92.26%) is higher than 70.0%, and its SO_3 and Cl contents (0% and 0.092%) are lower than 3.0% and 0.1%, respectively. Furthermore, the pozzolanic activity test results (1.43 MPa flexural strength and 6.12 MPa compressive strength) provide the requirements of T.S. 25, which are ≥1 and 4 MPa, respectively. XRD patterns have shown that (Fig. 2) ED contains cristobalite, quartz, feldspar, and an amorphous compound, and (ED)T has hydration products, cristobalite, quartz, feldspar, portlandite, and an amorphous compound.

Solid KOH with a molecular weight of 56.1 g/mol was

Table 1. Oxide Composition of ED, quicklime, and hardened mortar (ED)T determined by XRF

	Quicklime (%)	ED (%)	(ED)T mortar (%)
SiO_2	–	75.289	58.934
Al_2O_3	–	15.991	11.510
Fe_2O_3	–	0.984	0.829
Na_2O	–	2.211	1.361
K_2O	–	3.026	2.408
CaO	85	1.222	21.377
CO_2	5	–	–
MgO	1.5	0.622	2.870
P_2O_5	–	0.072	0.077
TiO_2	–	0.149	0.148
MnO_2	–	0.047	0.050
Cr_2O_3	–	0.005	–
NiO	–	0.004	0.005
CuO	–	0.002	–
ZnO	2.23	0.002	0.006
Rb	–	0.006	0.007
SrO	–	0.015	0.019
V_2O_5	–	–	0.022
Y_2O_3	–	0.002	0.006
ZrO_2	–	0.010	0.015
Nb_2O_5	–	0.001	0.008
BaO	–	0.097	0.075
Cl	–	0.092	0.078
SO_3	0.8	0.1	0.194
PbO	–	–	–
ThO_2	–	–	–
L.O.I.	–	0.15	–
Total	93.8	100.00	–

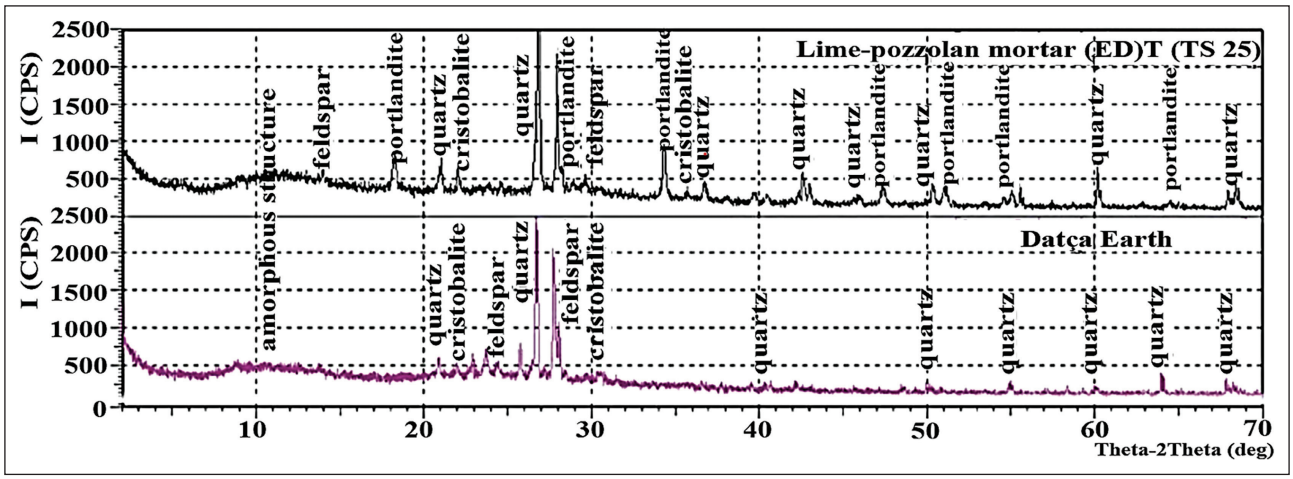


Figure 2. XRD data of ED and hardened mortar (ED)T.

dissolved in deionized water for 24 hours before use and kept at ambient temperature. The mass of solid KOH in the solution is expressed as Molar (M). 12.5 molar KOH solution contains 12.5 x 56.1=701 grams of solid KOH in a one–liter solution. The sodium silicate solution's molar ratio (SiO_2/Na_2O) is 3.4. Finely ground silica sand with 211 µm maximum grain size and 2.63 g/cm^3 specific gravity and aluminum powder foaming agent with 99% purity and 50 µm mean particle diameter was supplied from Ytong A.Ş.

2.2. Mixing, Molding, and Curing Process

The effects of activator types (NaOH, KOH, S+NaOH, and S+KOH), molar concentrations of the NaOH and KOH (7.5, 10, 12.5, and 15), and activator ratio (1.0, 1.5, 2.0, 2.5, by weight) on the geopolymeric reactivity were investigated in the previous research [26]. The combination of sodium silicate solution with potassium hydroxide (SK) as the activator type; 12.5 M as the concentration of KOH, and 2.5 as the activator ratio was selected for their better performance gain in physical and mechanical properties. In this research, the effectiveness of the following parameters, which may affect the development of the physical, mechanical, and thermal properties of the natural pozzolan–based geopolymer foam, was investigated:

i The effect of acceptable sand–to–pozzolan ratio (FS/P);
ii The effect of Al powder–to–pozzolan ratio (Al/P).

Fine aggregate/filler is generally not added to highly porous geopolymers having low thermal conductivities in the literature [3, 9–10, 13–16, 19–21]. It converts cementitious binders to mortars, gives mortars their volumetric stability, rigidity, and stiffness [27], and has a restraining effect on drying shrinkage due to the stability in shape [28]. Acceptable sand use as a filler may also decrease the production cost by reducing the amount of binder (pozzolan and chemical activators). In the preliminary tests of this research, and was not added to the ED–based geopolymer binder. The new binder expanded approximately 3.5 times within 10 minutes after the binder was poured

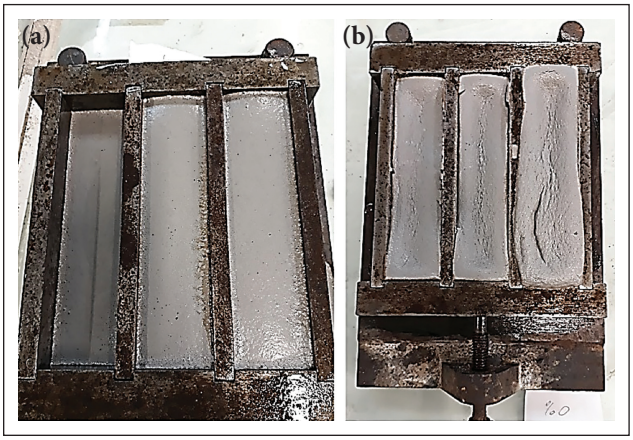


Figure 3. **(a)** The specimens 10 minutes after placing the molds; **(b)** The existence of collapse 30 minutes after placing the molds.

into the molds (Fig. 3a). However, after 30 minutes, separation of solid and gas phases was observed, and the foam collapsed (Fig. 3b). The reason for this result may be the lower plastic density (≤0.5 g/cm^3) of the porous binder which results in a significant decrease in the bubble confinement force (Fc) and leads to more giant and more closely spaced bubbles. Increasing bubble diameter causes an increase in the bubble buoyancy force (Fb). When Fb overcomes the surrounding Fc, bubbles become buoyant and float towards the surface of the porous binder, displace the surrounding solids, reach the surface, and collapse occurs [29]. Thus, in the first stage, the effects of the FS/P ratio (20/100, 25/100, 33/100, 50/100, and 100/100, by weight) on the properties of the foam were researched. The Al/P ratio was kept constant at 0.5% in this stage. The workability of the binder was determined by the flow table test performed according to ASTM C 1437 [30]. The water/total solid ratio, which results in optimum workability, was 0.4, and flow was found to be 100.

Table 2. The specimen codes, mixing ratios, and curing conditions of the ED-based geopolymer foams according to the experiment stages

Stage	Code	Activator ratio	Activator-to-pozzolan (*by weight*)	Total water-to-solid (*by weight*)	FS/P (*by weight*)	Al/P (%, *by weight*)	Curing conditions
i	SK-20/100-0.5	2.5	0.3	0.40	20/100	0.5	
	SK-25/100-0.5				25/100		
	SK-33/100-0.5				33/100		
	SK-50/100-0.5				50/100		
	SK-100/100-0.5				100/100		70 °C,
ii	SK-20/100-0	2.5	0.3	0.40	20/100	0	95±5 %
	SK-20/100-0.25					0.25	R.H. for
	SK-20/100-0.5					0.5	24 h
	SK-20/100-1.0					1.0	
	SK-20/100-1.5					1.5	

Specimen codes consist of XX-X-X format. The first symbol shows the alkali activator type (S: Sodium silicate, K: Potassium Hydroxide); the second shows the FS/P ratio, and the third points out the Al/P ratio.

According to the results of the first stage experiments, the FS/P ratio was selected as 20/100 because it has consistent properties for the following study stage. In the second stage, the effects of the Al/P ratio (0, 0.25, 0.50, 1.0, and 1.5%, by weight) on the foam's physical, mechanical, and thermal properties were tested. The specimen codes, mixing ratios, and curing conditions according to the experiment stages are shown in Table 2.

The solid components (ED and fine sand) were mixed in a plastic bowl and then added to previously homogenized alkali activators and mixed for 5 minutes. Afterward, Al powder was added and mixed for additional 2 minutes. The mixture was then poured into 40 x 40 x 160 mm molds. It should be noted that foaming started immediately after Al powder was added to the mix. The reaction time for volume expansion of the mixture took approximately 10 minutes. Since the volume expansion ratio of the foam differs depending on the quantity of the added Al powder, in each increment of the Al powder addition, the volume expansion ratio of the mortar was determined by using a 500 ml glass test tube. The produced fresh mortar was filled in this test tube up to the level of 100 ml. After the expansion was completed, the volume expansion ratio (R_{ve}) was calculated by Eq. (1):

$$R_{ve}=(V_f-V_i)/V_i \quad (1)$$

where Vi is the initial volume of the fresh mortar (ml); Vf is the final volume of the mortar (ml). Thus, the least amount of mixture was poured into the molds, and overflowing of the mixture from the mold during the expansion was prevented. The molded blend was covered with Polyethylene (P.E.) film to prevent rapid evaporation and cured at 70 °C and 95±5% R.H. for 24 h. Cured specimens were then taken from the oven and were kept at ambient temperature (20±2 °C, 50±5% R.H.) for seven days.

2.3. Testing Methods

Throughout the study, the relevant standards applied each physical and mechanical test to 9 prismatic specimens of 4 x 4 x 16 cm dimensions.

Bulk density was calculated as the ratio of the dry mass to volume of the samples dried to a constant weight in a ventilated oven at 105 °C (TS EN 1015–10 [31]).

The water absorption ratio (A_b) was calculated by considering the amount of water absorbed by the specimens, which were dried to a constant mass (m_d). The specimens were wholly immersed in water at 20°C for 48 hours, removed from the water, and weighed again (m_s). The water absorption ratio was calculated according to the following equation (2) (TS EN 13755 [32]):

$$A_b=([m_s-m_d]x100)/m_d \quad (2)$$

The ultrasound pulse velocity (U.P.V.) test was applied according to TS EN 14579 [33] with a portable Proceq ultrasonic non–destructive device.

The flexural strength was specified by using a machine (Universal) with a 300 kN capacity and 50 N/s loading rate (TS EN 196–1 [34]). The specimen was put on the machine with one side face on the supporting rollers and its longitudinal axis normal to the supports. The load was applied vertically using the loading roller to the opposite side face of the specimen and increased until fracture. The flexural strength (Rf) was according to the following equation (3):

$$R_f=(1.5xF_fxl)/b^3 \quad (3)$$

where b is the side of the square section of the specimen, (mm); Ff is the load applied to the middle of the specimen at fracture, (N); l is the distance between the supports, (mm).

Eighteen samples, broken into two pieces in the flexural strength test, were subjected to the compressive strength test (TS EN 196–1 [34]). The specimen was centered laterally to the machine's plates, and the load was increased at a 2400 N/s rate until fracture. Compressive strength (R_c) was calculated from Eq (4):

Table 3. Test results of the ED-based geopolymer foam

Stage	Code	Bulk density (g/cm^3)	Water absorption by weight (%)	Porosity (%)	UPV (km/s)	Flexural strength (MPa)	Compressive strength (MPa)
i	SK-20/100-0.5	0.51	69.63	76.80	1.25	0.90	1.39
	SK-25/100-0.5	0.55	66.09	72.72	1.28	1.02	1.63
	SK-33/100-0.5	0.59	59.15	70.62	1.32	1.15	1.76
	SK-50/100-0.5	0.64	54.04	68.47	1.44	1.37	1.95
	SK-100/100-0.5	0.85	48.02	64.01	1.60	1.62	2.52
ii	SK-20/100-0	1.29	28.69	43.72	1.95	3.92	5.69
	SK-20/100-0.25	0.60	63.68	72.31	1.41	1.22	2.09
	SK-20/100-0.5	0.51	69.63	76.80	1.25	0.90	1.39
	SK-20/100-1.0	0.48	74.75	79.69	0.91	0.33	0.85
	SK-20/100-1.5	0.46	79.32	82.66	0.65	0.12	0.40

$$R_c=(F_c/1600) \quad (4)$$

where Fc is the maximum load at fracture, (N); 1600 is the area of the plates (40 mm × 40 mm), (mm^2).

Thermal conductivity was measured using the heat flow meter apparatus in steady–state conditions per ASTM C518–17 [35]. The heat flow meter apparatus consists of two copper plates, one heat flux transducer, and a protective casing with thermal insulation to prevent heat loss. The specimen (100 mm diameter and 10 mm thickness) was positioned between two copper plates, and the heat flow passing through the plates was recorded. The difference in temperature between the copper plates ($\Delta T=T_1-T_2$) and the heat flux (Q) was obtained with conventional sensors. Fourier's law of heat conduction was used to calculate thermal conductivity by using Eq. (5):

$$Q = \lambda \frac{\Delta T}{\Delta x} = \lambda \frac{T1 - T2}{d} \quad (5)$$

where Q is heat flux flowing through the specimen (W/m^2), λ is thermal conductivity (W/mK), ΔT is the temperature difference across the specimen (K), x and d are the thickness of the specimen (m), T/x is temperature gradient (K/m).

Optical analysis, which gives a detailed two–dimensional picture of the pores, was carried out to characterize the morphology of macroscale pores (>10 μm). The specimens were cut from geopolymer foams using a cutting machine. Three samples were prepared for each analysis, and four images of a fracture section of each sample were observed by optical microscope (1×). However, it is difficult to determine the pore size distribution solely by analyzing the microscopic images. Therefore, image analysis was conducted using Image–Pro Plus Image Analysis Software to analyze better the morphology of macroscale pores (air pores with >10 μm). The pore dimensions were quantified with equivalent circle diameter. Porosity, average pore diameter, maximum pore diameter, and pore size distribution were determined. The distribution of mesoscale pore (100 nm –10 μm) was not considered because they are assumed to be insignificant in affecting the properties of geopolymer foams [36]. The test results are given in Table 3.

3. RESULTS AND DISCUSSION

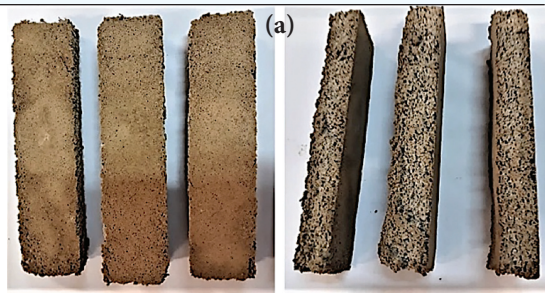
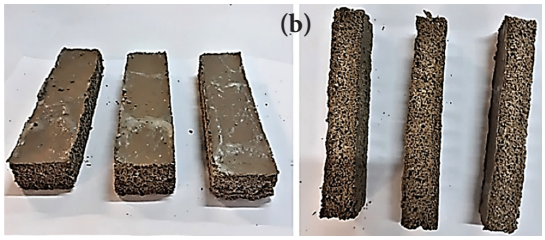
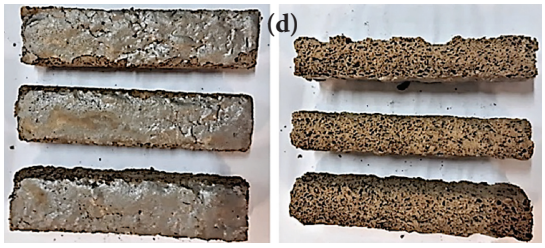
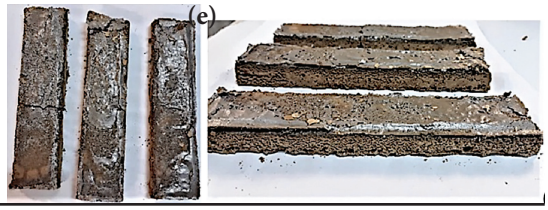
3.1. Influence of the Fine Sand–to–Pozzolan Ratio on the Properties of the ED–Based Geopolymer Foam

Pores are generated by a gas–releasing reaction in the geopolymer mixture, which results in a cellular structure when set. After Al powder is added to the homogeneous geopolymer mixture, in the alkali environment, reactive metal powders are oxidized in the presence of water to release H_2 gas according to the reaction in Eq. (6) [37]:

$$Al\,(s)+3H_2O(l)+OH^-(aq)\rightarrow Al(OH)^{-4}\,(aq)+3/2H_2\,(g) \quad (6)$$

The hydrogen gas bubbles generated led to the ED–based geopolymer binder's expansion, which continued for the next 10 minutes. The influence of the FS/P ratio on the volume expansion ratio of the mortar was investigated together with the observation of the surface properties of the expanded specimens (Table 4). According to this, the volume of the first series prepared with a 20/a 100 FS/P ratio increased 3.0 times compared to their initial volume. Volume expansion ratios of the specimens, for each fine sand–pozzolan ratio increment, decreased by 2.8, 2.5, 2.2, and 1.1 times respectively. Especially in the specimens with the highest sand content (100/100 FS/P ratio), Al powder could not swell the binder, and almost no volume expansion (Table 4–Fig. e). The higher the amount of sand, the lower the alkali activator, Al powder, and pozzolan ratio, which are responsible for foaming the binder. In addition, light gray material precipitation looking like aluminum was observed on the top open surfaces of the sand–rich specimens (33/100, 50/100, and 100/100 FS/P ratio) after oven curing at 70 °C. This causes surface deformation; accordingly, the color and texture homogeneity of the specimens was impaired (Table 4–Fig. c–e).

Table 4. The effects of the FS/P ratio on the volume expansion ratio and surface properties of the swollen specimens

FS/P (*by weight*)	Volume expansion ratio	Surface properties	The specimens after 70 °C ovens curing for 24 h
20/100	3.0 times	Homogenous surface and color	
25/100	2.8 times	Homogenous surface and color	
33/100	2.5 times	Non-homogenous surface and color	
50/100	2.2 times	Non-homogenous surface and color	
100/100	1.1 times	Non-homogenous surface and color	

The influence of the FS/P ratio on the physical and mechanical properties of ED–based geopolymer foam is given in Figure 4.

The gradual increase of the FS/P ratio from 20 to 100% decreased porosity and water absorption by 0.83 and 0.68, respectively. Parallel to this decrease, there was an almost twofold increase in the bulk density of the specimens (1.66 times). Notably, this becomes significant in the region between 50 to 100% FS/P ratio, where the increment ratio of the sand is twofold. U.P.V., flexural and compressive strengths of the specimens increased 1.28, 1.80, and 1.81 times, respectively. When the increment of the sand ratio is twofold in the region between 50 to 100% FS/P ratio, the material's compressive strength increases significantly parallel to the increase of its bulk density.

Figure 5 shows the microscopic images of ED–based geopolymer foams in each FS/P ratio. The sand ratio increases lead to a decrease in the pore volume (porosity) and the number of pores, which is also consistent with physical

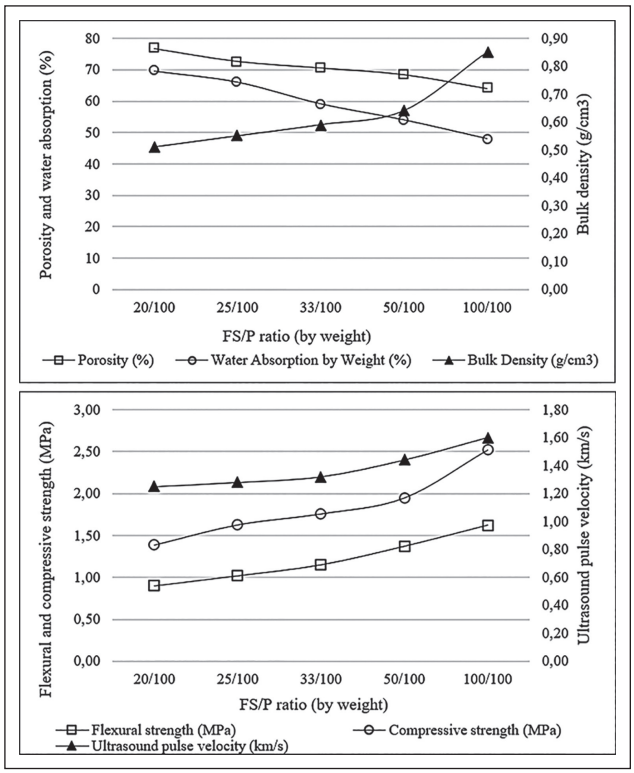


Figure 4. Effects of the FS/P ratio on the physical and mechanical properties of ED-based geopolymer foam.

test results. Frequency distribution diagrams of the pore diameters were prepared and given in Figure 6. Accordingly, the diameter of the specimens' pores ranged from 61 μm to 2038 μm (2.038 mm). The gradual increase of the FS/P ratio from 20/100 to 100/100 reveals that the distribution of pore size shifts towards the larger pore size distribution. The specimens with a 20/100 FS/P ratio are more homogenous with finer pore sizes, regular (narrower) pore size distribution, and a maximum 1217 μm pore diameter. When the sand content of the binder increases, the porous matrix shows the non–homogeneous distribution of larger pores, and the maximum pore diameter increases up to 2038 μm. The average pore diameter is 280 μm in the specimens having a 20/100 FS/P ratio, while the average pore diameter increases up to 407 μm depending on the increase of the FS/P ratio (100/100). These findings may be due to a higher proportion of pores between fine sand particles and at the fine sand–binder interface. In addition, the pores of sand–rich specimens have a higher degree of interconnectivity, whereas the specimens having lower sand content have a relatively lower degree of interconnectivity between pores. Furthermore, while the number of pores per mm^2 is the highest in samples with a 20/a 100 FS/P ratio, increasing sand content decreased the number of pores per mm^2. From these findings, it can be inferred that the total amount of fine sand in the porous geopolymer mixture controls the pores' total volume, dimension, and size distribution.

Total pore areas and porosities of the specimens as a function of the FS/P ratio are given in Figure 7. According to this, both the porosities of the specimens (obtained by experiments) and total pore areas per mm^2 (obtained by image analysis) decrease with the increase of sand content of the mixture. This decreasing trend is significantly similar for both factors, which may also denote that the image analysis is a suitable method for determining the pore volume of the geopolymer foams.

3.2. Influence of the Al Powder–to–Pozzolan Ratio on the Properties of the ED–Based Geopolymer Foam

The effects of the Al/P ratio on the physical and mechanical properties of ED–based geopolymer foam having 20% find sand content are given in Figure 8.

When the Al/P ratio increases gradually from 0% to 1.5%, two distinct regions become apparent in the evolution of the properties. At first, adding 0.25% Al/P into the mixture was quite effective in pore–forming, and the bulk density of the material dropped by 53%. Beyond this level to the 1.5% Al/P, even though there was a 1.25 times increment in the Al powder ratio, the same property only decreased by 23%, which may show the influence of Al powder in pore–forming became lower. Other properties of the material as a function of Al/P ratio increment displayed almost a coherent change with the bulk density. At 0.25% Al/P ratio, the porosity, and the water absorption ratio increased sharply by 1.65 and 2.21 times, and parallel to this increase in U.P.V., flexural and compressive strengths of the specimen decreased by 0.72, 0.31, and 0.36 times, respectively. The gradual decrease in U.P.V. (54%) in the whole aluminum powder increment range may have resulted from the porous structure's gradual formation. The decreasing tendency of physical and mechanical properties with the increasing pore foaming agent content is also consistent with other study results [3, 5, 38].

Figure 9 shows the microscopic images of ED–based geopolymer foams with various Al/P ratios, and Figure 10 shows frequency distribution diagrams of the pore diameters and average and maximum values of pore diameters of ED–based geopolymer foams with various Al/P ratios.

Increasing the Al/P ratio from 0 to 1.5% led to an increase in the total pore volume of the ED–based geopolymer and was consistent with the physical test results (Fig. 9 and 10). Pore diameters of the specimens ranged between 72 μm and 1787 μm (1.787 mm). Specimen with 0.25% Al/P ratio has homogenous, fine pore size with regular (narrower) pore size distributions. Average and maximum pore diameter was detected as 268 μm and 1200 μm, respectively. Gradually increase in the Al/P ratio from 0.25 to 1.5% shifted the pores of the specimen towards broader pore size distribution. Non–homogeneous distribution of larger pores with an average pore diameter of 411 μm and maximum pore diameter of 1787 μm were detected in its porous matrix. In addition, the pores showed a higher degree of interconnectivity than the specimens, with a 0.25%

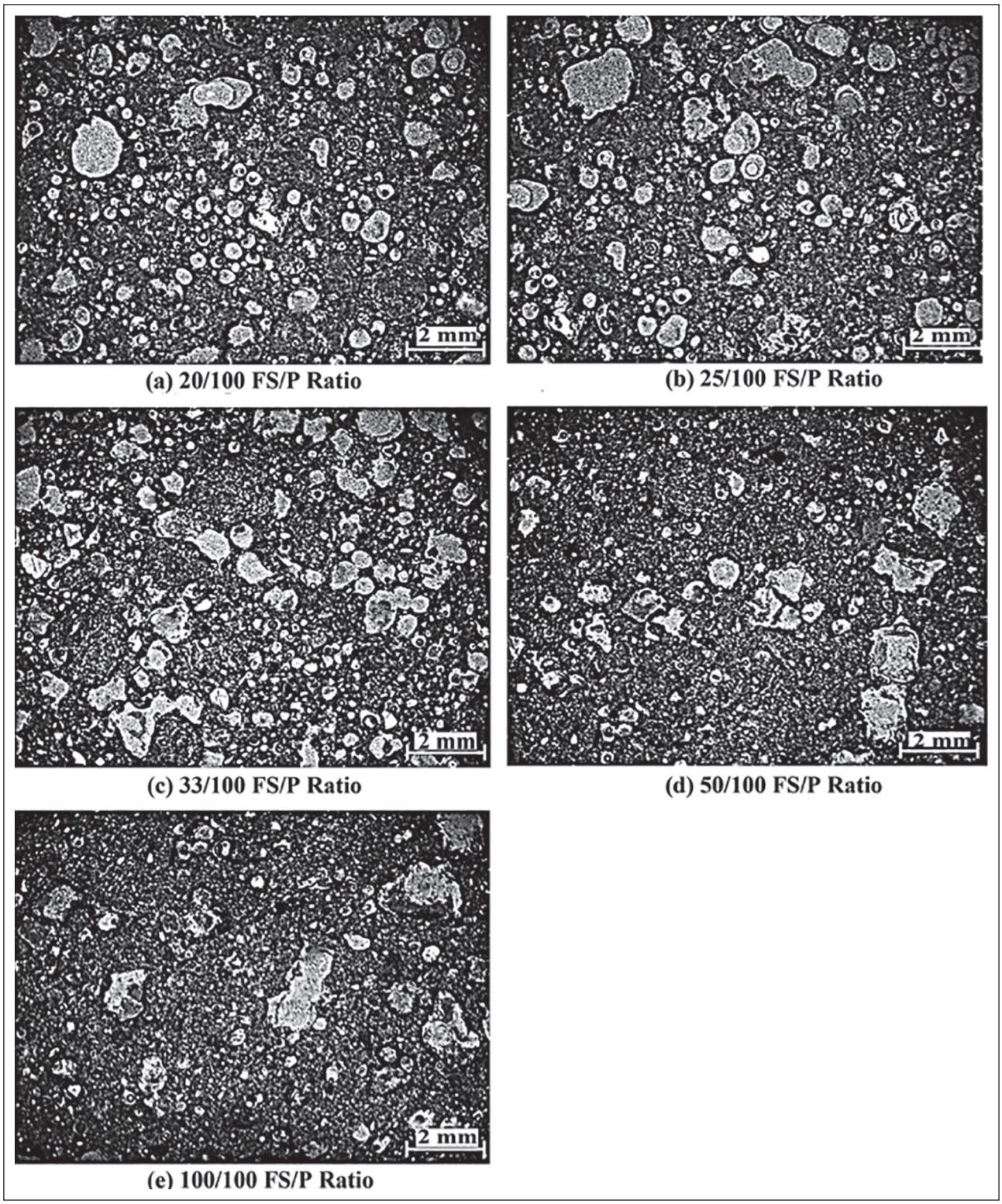


Figure 5. Microscopic images of ED-based geopolymer foams having various FS/P ratios.

Al/P ratio. This degree of pore coalescence may have led to a non–homogeneous pore structure and caused the least number of pores per mm^2, compared to other samples. Similar results were obtained by various studies [16, 39]. Thus, it can be stated that in the porous geopolymer mixtures, the content of Al powder is decisive in determining the total volume, dimension, size distribution of the pores, and the degree of interconnectivity between them.

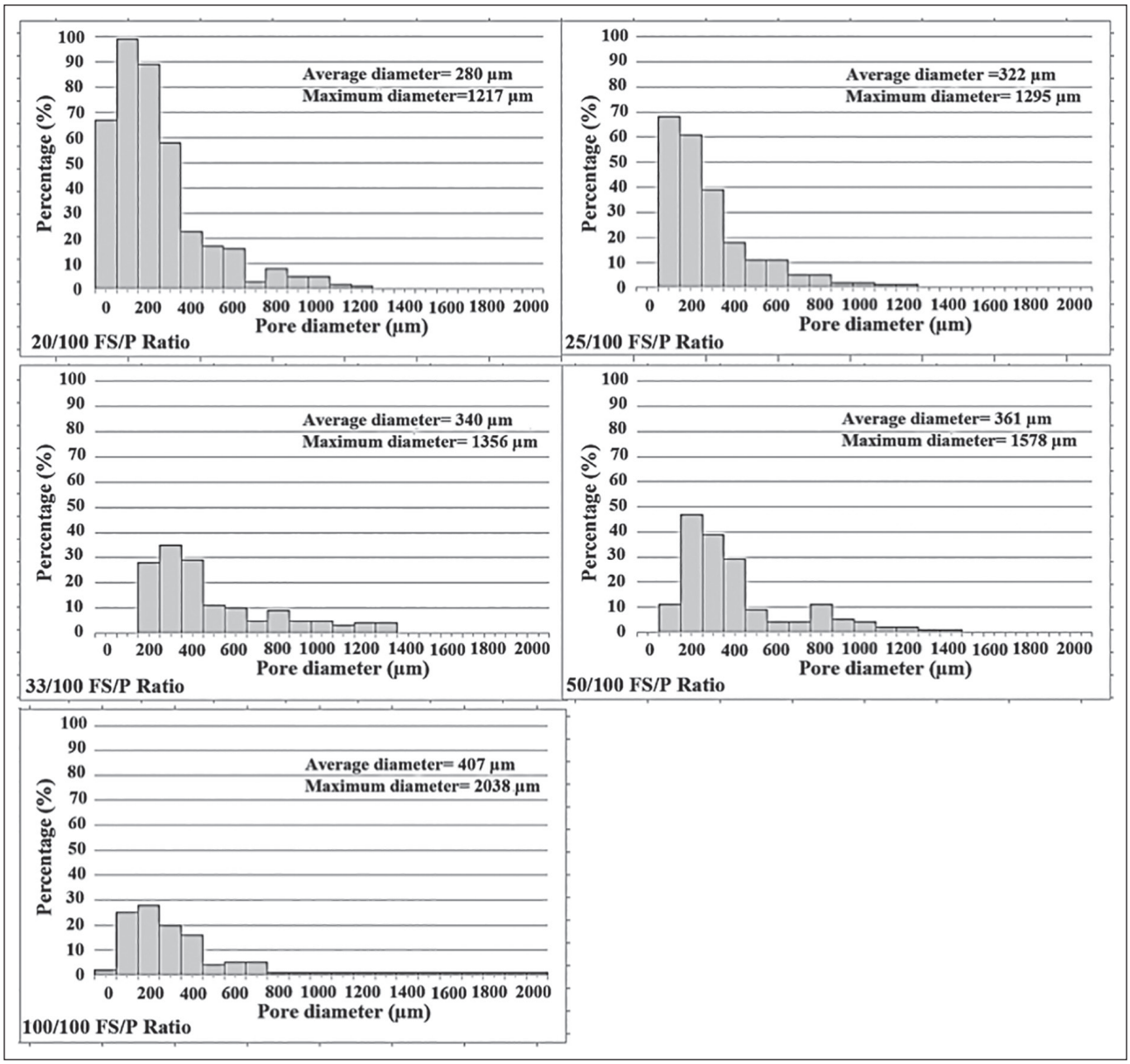


Figure 6. Frequency distribution diagrams of the pore diameters, average and maximum values of pore diameters of ED-based geopolymer foams having various FS/P ratios.

The ultrasound pulse velocity (U.P.V.) is a non–destructive test method used to measure the homogeneity of concrete [40]. The pores and cracks in the concrete reduce the U.P.V. of the material, which aids in specifying the quality of concrete [41]. In this study, the homogeneity of the pore distribution of the material is determined by measuring the U.P.V. in two different regions of the sample (Fig. 11a), and the homogeneity percentage is calculated according to the standard deviation of U.P.V. results (Fig. 11b). The highest homogeneity (99.3%) was obtained from the specimens which do not have any Al powder content as expected. Increasing the Al powder content led to a decrease in the homogeneity of the ED–based geopolymer

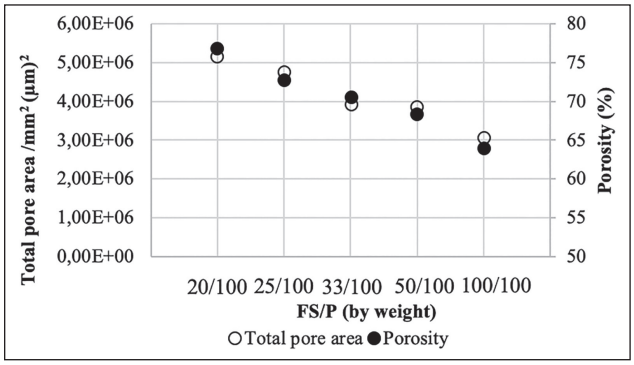


Figure 7. Total pore area and porosity of ED-based geopolymer foams as a function of FS/P ratio.

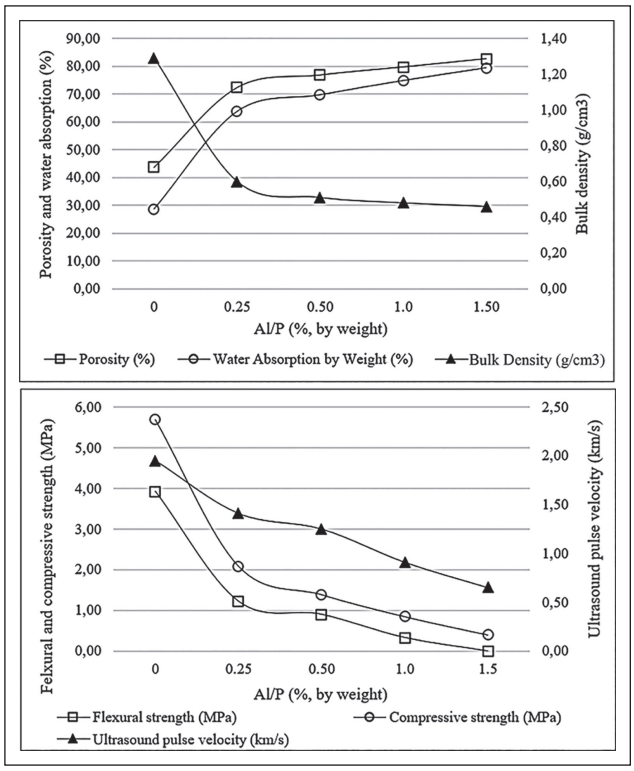


Figure 8. Effects of Al/P ratio on the physical and mechanical properties of ED-based geopolymer foam.

foams. Mainly, the least level of homogeneity (85.8%) was observed in the specimens having a 1.5% Al/P ratio, which may have resulted from the larger pore size distribution. This result confirms the findings that adding more Al powder may cause a microstructure with larger pores and irregular pore size distribution.

The effects of the Al/P ratio on porosity, average pore diameter, thermal conductivity, and compressive strength are given in Figure 12.

The porous microstructure of ED–based geopolymer mortar by adding Al powder in various proportions caused lower compressive strength than the sample without Al powder content. The specimens containing lower amounts of Al powder (0.25 and 0.50%) have found higher strengths due to the paste's being more homogenous with finer pore size and narrower pore size distribution. In addition, these specimens have a relatively lower amount of interconnectivity between pores. Thus, regularly formed air pores increase the compressive strength [42]. However, in the specimens with a 1.5% Al/P ratio, pores were interconnected, and a higher degree of pore interconnectivity and foam coalescence (merging of bubbles) led to a wide distribution of pore size and lower strength [42]. When the pore wall is too thin to bear incoming shrinkage, and if there are excessive bubbles in the matrix, during the drying process, the films between them become weak, and the bubbles start to co-

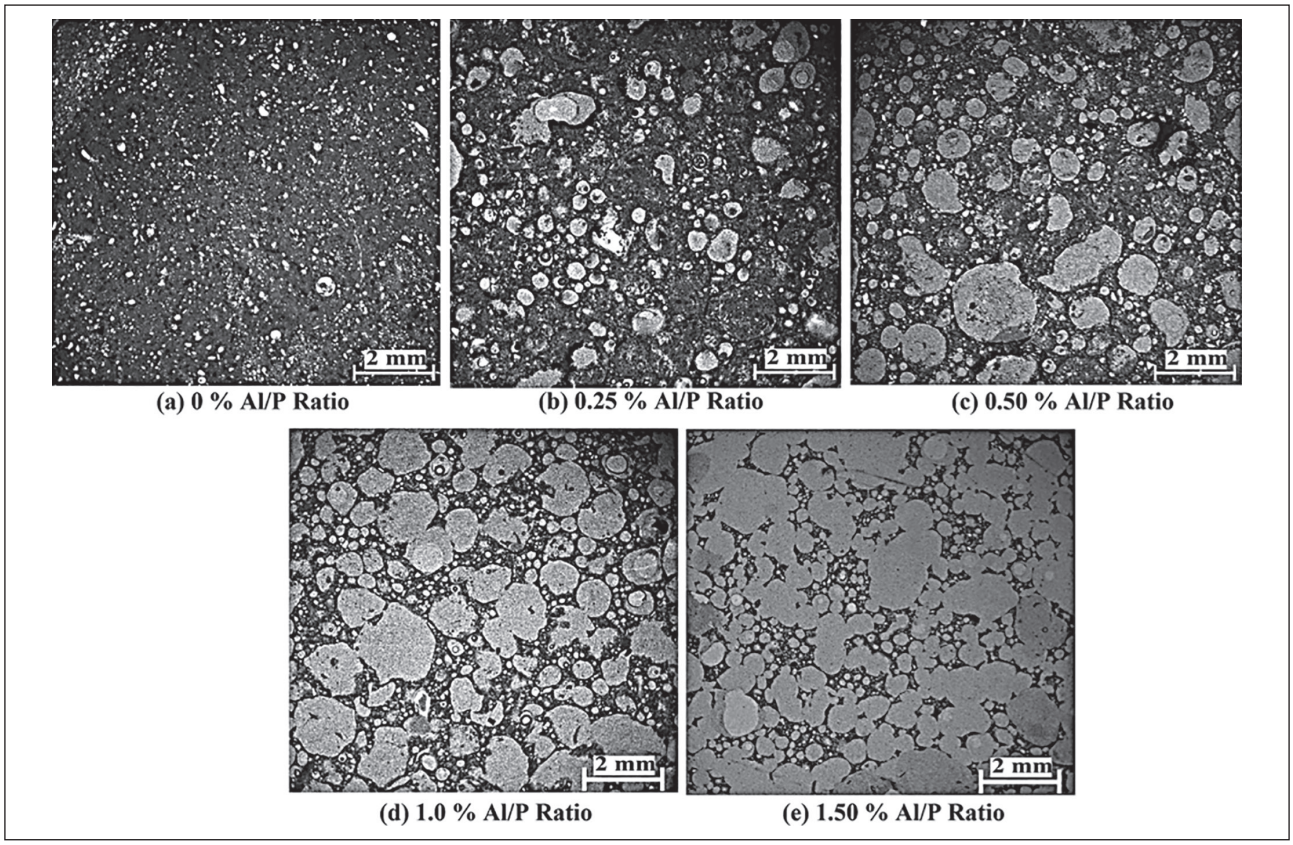


Figure 9. Microscopic images of ED-based geopolymer foams having various Al/P ratios.

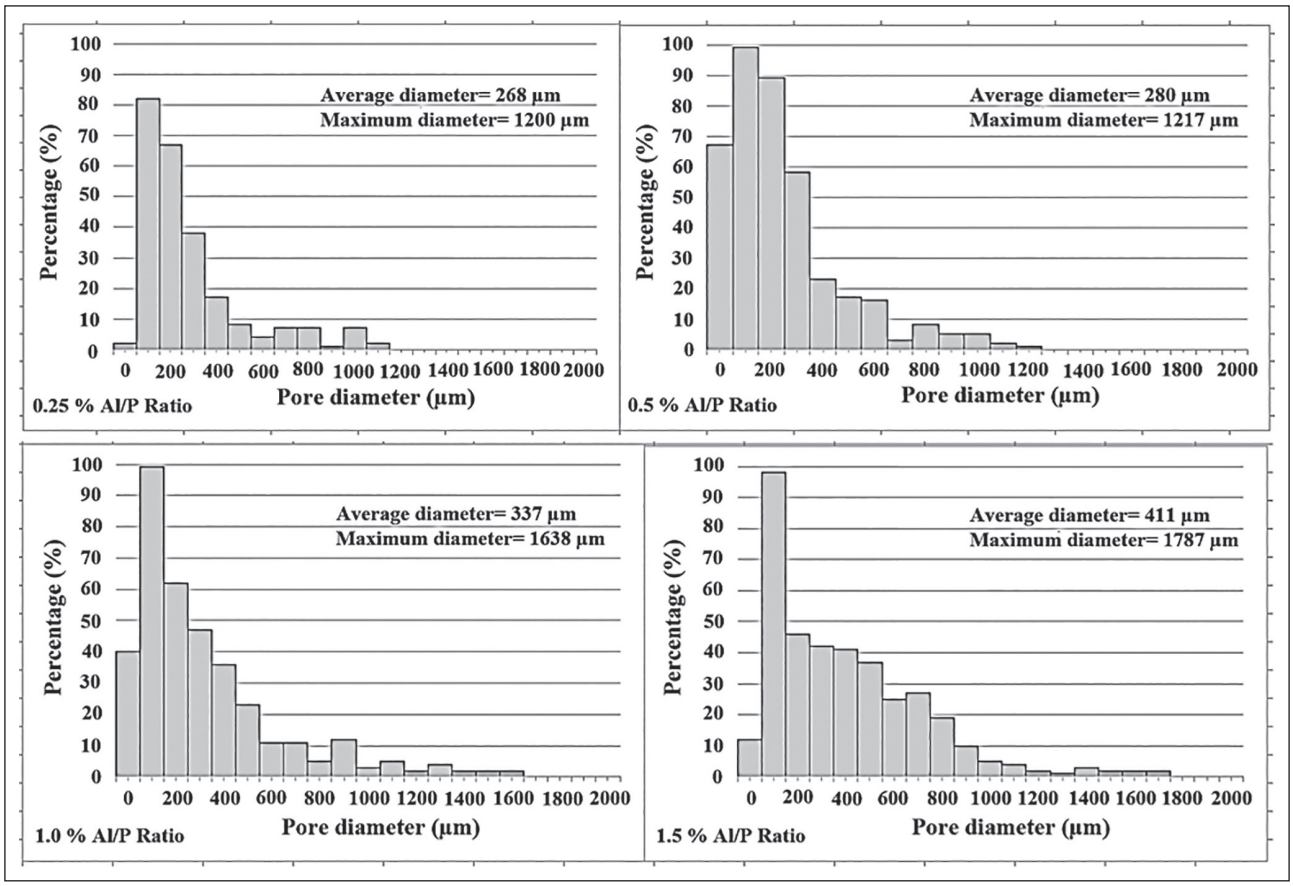


Figure 10. Frequency distribution diagrams of the pore diameters, average and maximum values of pore diameters of ED-based geopolymer foams having various Al/P ratios.

alesce, giving rise to much more connected pores with larger overall pore size. Accordingly, the mechanical properties of the material decrease [43–46].

3.3. Thermal Properties of the ED–Based Geopolymer Foam

In the current study, Al powder was added to the geopolymer mortar to reduce its thermal conductivity without compromising the physical and mechanical performance requirements required for the material to be used in partition walls. The gradual increase of the Al/P ratio from 0% to 1.5% is directly proportional to the increase in porosity (1.89 times), but it is inversely proportional to the thermal conductivity, where it decreased from 0.312 W/mK to 0.087 W/mK (0.27 times) (Figure 12). A higher degree of porosity means more pores that may act as thermal insulation [47] since the thermal conductivity of still–air is lower than that of the solid matrix [48]. The most significant decrease in the thermal conductivity of the material occurred between 0–0.25% Al/P ratio, which highlights the positive effect of Al powder addition on lowering the thermal conductivity of the solid matrix. By increasing the Al/P ratio from 0.25 to 0.50, the porosity and average pore diameter increased approximately 1.1 times, while the thermal conductivity decreased 0.75 times. By increasing the Al/P ratio from 0.50 to 1.50, although the porosity and pore diameter increased approximately 1.50 times, the decrease in the thermal conductivity was only 0.86 times (Figure 12). Increasing the amount of Al/P ratio by more than 0.50 did not give the expected effect in reducing the thermal conductivity. This may be due to the contrasting effect of the non–homogeneous pore size distribution with larger pores (Figure 9). Therefore, it can be stated that the development of the thermal insulation capacity of a geopolymer foam is not only affected by the porosity and hence density, but also by the pore size, shape, and interconnectivity between pores [49, 50]. Smaller, more circular, and less interconnected pores increase the insulation capacity in porous structures [51].

In the case of higher thermal performance is expected, the specimen with the lowest thermal conductivity (0.087 W/mK) having the highest Al/P ratio can be selected as optimum. However, mechanical properties cannot be ignored during practical implementations [43]. Indeed, it is expected that these porous materials have the least strength that could maintain their stability under loads of non–load bearing wall sections. The criteria in the production of ED–based geopolymer foam are determined to have a thermal

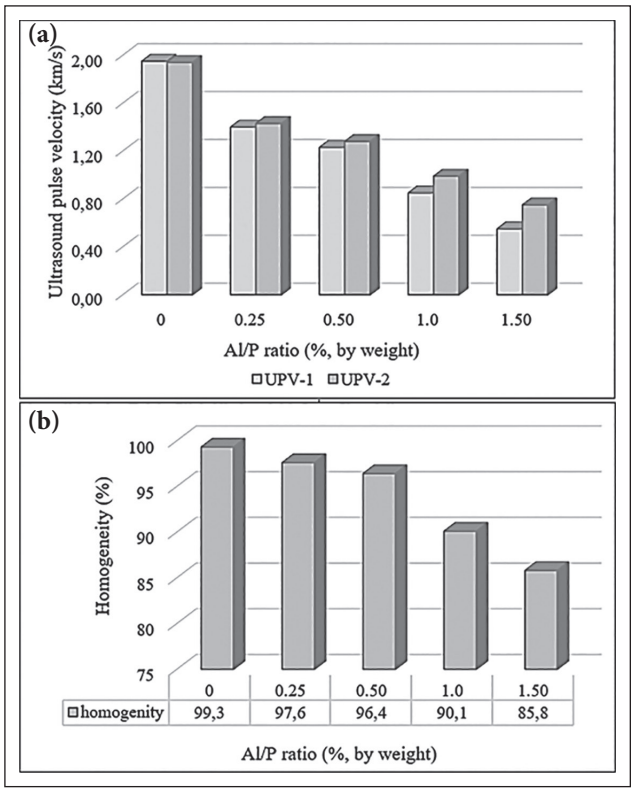


Figure 11. **(a)** Ultrasound pulse velocity obtained from two different regions in a sample; **(b)** calculated homogeneity percentage.

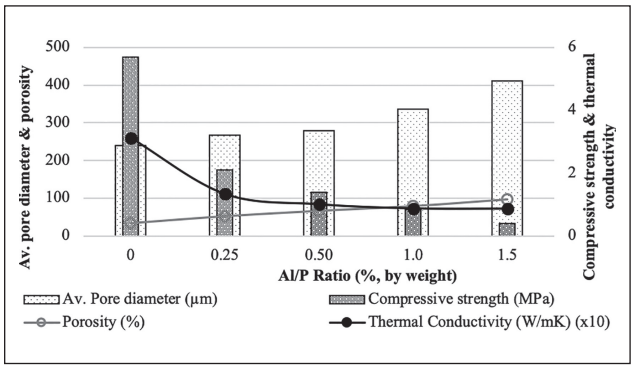


Figure 12. Effects of the Al/P ratio on porosity, average pore diameter, thermal conductivity, and compressive strength.

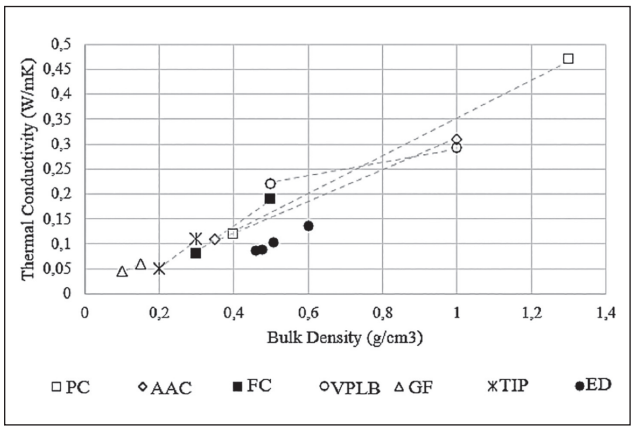


Figure 13. Comparison of the properties of ED-based geopolymer foam with inorganic ceramic wall and insulation materials (P.C.: Pumice concrete, A.A.C.: Aerated autoclaved concrete, F.C.: Foam concrete, VPLB: Vertically lightweight perforated brick, G.F.: Glass foam, T.I.P.: Thermal insulation plasters, ED: Earth of Datça-based geopolymer foam).

conductivity of ≤0.1 W/mK and compressive strength of ≥1.0 MPa [48]. According to this, the optimum Al/P ratio of 0.5% meets the determined criteria.

3.4. Comparison with Other Current Inorganic Ceramic Wall and Insulation Materials

Bulk density, thermal conductivity, and compressive strengths of ED–based geopolymer foams are compared with those of various inorganic ceramic wall and insulation materials used in the building sector (Table 5, Fig. 13).

According to Table 5 and Figure 13, the thermal conductivities of ED–based geopolymer foams produced in this study were higher than that of glass foam and lower than that of vertically perforated lightweight brick; similar results were obtained with pumice concrete, aerated autoclaved concrete, and foam concrete. Suppose protective layers can compensate for their lower compressive strength and higher water absorption ratio. In that case, this material may be used as a core layer of a laminated geopolymer composite, which behaves homogenously regarding macro scale.

3.5. Comparison with Other Existing Studies in the Literature

The porosity, thermal conductivity, and compressive strength of ED–based geopolymer foams are compared with those of geopolymer foams produced from various aluminosilicate sources and pore foaming agents (Table 6).

According to this comparison, the lowest thermal conductivity of ED–based geopolymer foam (0.087 W/mK) is higher than that of ultrafine perlite–based geopolymer foam [9]; similar to that of fly ash [3], bottom ash [20, 53], and a combination of metakaolin and fly ash [54] based foams; lower than that of fly ash [10, 38], calcined kaolin [55], natural soil of Pakistan [5], a combination of metakaolin and silica fume [6], metakaolin [13, 14, 16, 56], waste glass [19], and metakaolin waste, glass waste and steel–plant waste [21]–based geopolymer foams. It is seen that the porosity and compressive strength values of the produced foam like to those of the other materials in the table. Thus, ED–based geopolymer foam looks promising to be used as a rigid inorganic wall insulation material in the building industry.

Table 5. Compare ED-based geopolymer foam properties with other inorganic ceramic wall and insulation materials

Material	Bulk density (g/cm^3)	Thermal conductivity (WmK)	Compressive strength (MPa)
Thermal insulation plasters [52]	≥0.2	0.05–0.10	–
Pumice concrete [52]	0.4–1.3	0.12–0.47	2.5–5.0
Aerated autoclaved concrete [52]	0.35–1.0	0.11–0.31	≥4
Foam concrete [10]	0.3–0.5	0.081–0.19	≥0.4
Vertically perforated lightweight brick [52]	0.5–1.0	0.22–0.29	2.5–7.5
Glass foam [52]	0.1–0.15	0.045–0.060	0.12–0.14
Earth of Datça-based geopolymer foam			
Al/P ratio (%)			
0	1.29	0.312	5.69
0.25	0.60	0.134	2.09
0.50	**0.51**	**0.101**	**1.39**
1.0	0.48	0.088	0.85
1.5	0.46	0.087	0.40

Table 6. Comparison of ED-based geopolymer foam properties with other geopolymer foams containing various aluminosilicate sources and pore-forming agents

Reference	Aluminosilicate source	Pore-forming agent	Porosity (%)	Thermal conductivity (W/mK)	Compressive strength (%)
[9]	Ultrafine perlite	H_2O_2	74–89	0.03–0.06	0.2–0.8
[3]	Fly ash	H_2O_2	74–81	0.07–0.09	0.4–1.4
[53]	Bottom ash	Sodium silicate	66–76	0.074–0.09	1.2–3.5
[20]	Bottom ash	Sodium silicate	42–73	0.075–0.091	3.0–6.2
[54]	Metakaolin+ fly ash	H_2O_2	48–81	0.08–0.2	0.3–21
Current study	**Earth of Datça**	**Al powder**	**72.3–82.6**	**0.087–0.134**	**0.40–2.09**
[10]	Fly ash	H_2O_2	41.5–72.5	0.10–0.40	1.2–6.6
[55]	Calcined kaolin	H_2O_2	56–75	0.11–0.17	1.8–5.2
[14]	Metakaolin	H_2O_2	60.2–83.1	0.11–0.17	0.3–11.6
[6]	Silica fume +metakaolin	Silica fume	78–85	0.12–0.17	–
[13]	Metakaolin	Silica fume	65–85	0.12–0.35	–
[56]	Metakaolin	Silica fume	65–85	0.12–0.35	–
[21]	Metakaolin waste, Glass waste, Steel-plant waste	Aluminum scrap recycling waste	83–86	0.14–0.15	1.1–2.0
[16]	Metakaolin	Al powder	30–70	0.15–0.60	–
[19]	Waste glass	H_2O_2	55	0.21	7.3
[5]	Natural soil from Pakistan	H_2O_2	54–63	0.27–0.35	1.57–2.41
[38]	Fly ash	SiC powder	32–52	0.42–0.67	1.2–4.1

4. CONCLUSIONS

In line with the results obtained throughout the study, the following remarks can be specified:

- Geopolymer mixture produced by mixing Al powder as a foaming agent and volcanic Tuff of Datça Peninsula in Turkey as aluminosilicate source gives promising results in producing highly porous geopolymers with low thermal conductivity.
- The addition of finely ground silica sand ensures the volumetric stability of the geopolymer binder and prevents the collapse after swelling of the binder.
- The volume expansion ratio of the binder decreases with the increasing fine sand to pozzolan (FS/P) ratio.

The optimum FS/P ratio is determined as 20/100 since it enables the production of more homogeneous mortar without any collapse and surface deformation. The pores of sand–rich specimens show the non–homogeneous distribution of the larger pores with a higher degree of interconnectivity. Furthermore, because fine sand decreases the porosity and increases the density of the mortar, it leads to reduce thermal performance; the amount of fine sand should not be increased unnecessarily.

- The optimum Al powder to pozzolan (Al/P) ratio is determined as 0.5% because it gives better physical, mechanical, and thermal properties due to its more homogenous microstructure with finer pore size, regular (narrower) pore size distribution, and lower degree of interconnectivity (low amount of pore coalescence).
- The thermal conductivity is affected by the total volume of the macroscale pores (>10 μm), shape, and interconnectivity between pores. Smaller, more circular, and less interconnected pores increase the insulation capacity in porous structures.
- Thermal conductivities of ED–based geopolymer foams (0.087–0.134 W/mK) were found within a similar range with commonly used alternative inorganic ceramic wall materials.
- The high insulation capacity is considered the main key parameter. ED–based geopolymer foam provided promising data to be used as a rigid wall insulation material in the building industry. However, its comparatively lower mechanical properties and higher water absorption ratio could be compensated by protective layers, and it could be used as a core layer of a laminated geopolymer composite that behaves homogenously with regard to macro scale.

ACKNOWLEDGMENTS

The authors express their gratitude to Prof. Dr. Emin Çiftçi, who provided the I.T.U. Department of Geological Engineering laboratory facilities for optical microscope analysis.

DATA AVAILABILITY STATEMENT

The authors confirm that the data that supports the findings of this study are available within the article. Raw data that support the finding of this study are available from the corresponding author, upon reasonable request.

CONFLICT OF INTEREST

The authors declare that they have no conflict of interest.

FINANCIAL DISCLOSURE

This research was financially supported by the Center for Scientific Research Projects of Istanbul Technical University [grant number MGA–2019–41837].

PEER–REVIEW

Externally peer–reviewed.

REFERENCES

[1] Liu, M.Y.J., Alengaram, U.J., Jumaat, M.Z., & Mo, K.H. (2014). Evaluation of thermal conductivity, mechanical, and transport properties of lightweight aggregate foamed geopolymer concrete. *Energy and Buildings*, 72, 238–245. [CrossRef]

[2] Allouhi, A., El Fouih, Y., Kousksou, T., Jamil, A., Zeraouli, Y., & Mourad, Y. (2015). Energy consumption and efficiency in buildings: current status and future trends. *Journal of Cleaner Production*, 109, 118–130. [CrossRef]

[3] Feng, J., Zhang, R., Gong, L., Li, Y., Cao, W., & Cheng, X. (2015). Development of porous fly ash–based geopolymer with low thermal conductivity. *Materials Design*, 65, 529–533. [CrossRef]

[4] Garcia–Lodeiro, I., Palomo, A., & Fernández–Jiménez, A. (2015). An overview of the chemistry of alkali–activated cement–based binders. In: Pacheco–Torgal F, Labrincha JA, Leonelli C, Palomo A, Chindaprasirt P (Ed,). *Handbook of Alkali–Activated Cements, Mortars, and Concretes*, Woodhead Publishing, U.K., 19–47. [CrossRef]

[5] Zaidi, S.F.A., Haq, E.U., Nur, K., Ejaz, N., Anis–Ur–Rehman, M., Zubair, M., & Naveed, M. (2017). Synthesis & characterization of natural soil based inorganic polymer foam for thermal insulations. *Construction and Building Materials*, 157, 994–1000. [CrossRef]

[6] Papa, E., Medri, V., Kpogbemabou, D., Morinière, V., Laumonier, J., Vaccari, A., & Rossignol, S. (2016). Porosity and insulating properties of silica–fume based foams. *Energy and Buildings*, 131, 223–232. [CrossRef]

[7] Duxson, P., Provis, J.L., Lukey, G.C., & van Deventer, J.S.J. (2007). The role of inorganic polymer technology in the development of 'green concrete'. *Cement and Concrete Research*, 37(12), 1590–1597. [CrossRef]

[8] Bai, C., & Colombo, P. (2018). Processing, properties and applications of highly porous geopolymers: A review. *Ceramics International*, 44(14), 16103–16118. [CrossRef]

[9] Vaou, V., & Panias, D. (2010). Thermal insulating foamy geopolymers from perlite. *Minerals Engineering*, 23(14), 1146–1151. [CrossRef]

[10] Novais, R.M., Buruberri, L.H., Ascensao, G., Seabra, M.P., & Labrincha, J.A. (2016a). Porous biomass fly ash–based geopolymers with tailored thermal conductivity. *Journal of Cleaner Production*, 119, 99–107. [CrossRef]

[11] Łach, M., Pławecka, K., Bąk, A., Lichocka, K., Korniejenko, K., Cheng, A., & Lin, W.T. (2021). Determination of the influence of hydraulic additives on the foaming process and stability of the produced geopolymer foams. *Materials*, 14, Article 5090. [CrossRef]

[12] Phavongkham, V., Wattanasiriwech, S., Cheng, T–W., & Wattanasiriwech, D. (2020). Effects of surfactant on thermo–mechanical behavior of geopolymer foam paste made with sodium perborate foaming agent. *Construction and Building Materials*, 243, Article 118282. [CrossRef]

[13] Henon, J., Alzina, A., Absi, J., Smith, D.S., & Rossignol, S. (2013). Potassium geopolymer foams made with silica fume pore forming agent for thermal insulation. *Journal of Porous Materials*, 20, 37–46. [CrossRef]

[14] Bai, C., Ni, T., Qiaoling, W., Hongqiang, L., & Colombo, P. (2018). Porosity, mechanical and insulating properties of geopolymer foams using vegetable oil as the stabilizing agent. *Journal of European Ceramic Society*, 38, 799–805. [CrossRef]

[15] Qiao, Y., Li, X., Bai, C., Li, H., Yan, J., Wang, Y., Wang, X., Zhang, X., Zheng T., & Colombo, P. (2021). Effects of surfactants/stabilizing agents on the microstructure and properties of porous geopolymers by direct foaming. *Journal of Asian Ceramic Societies*, 9(1), 412–423. [CrossRef]

[16] Kamseu, E., Nait–Ali, B., Bignozzi, M.C., Leonelli, C., Rossignol, S., & Smith, D.S. (2012). Bulk composition and microstructure dependence of effective thermal conductivity of porous inorganic polymer cements. *Journal of European Ceramic Society*, 32(8), 1593–1603. [CrossRef]

[17] Peng, X., Li, H., Shuai, Q., & Wang L. (2020). Fire resistance of alkali activated geopolymer foams produced from metakaolin and Na_2O_2. *Materials (Basel)*, 13(3), 535. [CrossRef]

[18] Sornlar, W., Wannagon, A., & Supothina, S. (2021). Stabilized homogeneous porous structure and pore type effects on the properties of lightweight kaolinite–based geopolymers. *Journal of Building Engineering*, 44, Article 103273. [CrossRef]

[19] Bai, C., Li, H., Bernardo, E., & Colombo, P. (2019). Waste–to–resource preparation of glass–containing foams from geopolymers. *Ceramics International*, 45(6), 7196–7202. [CrossRef]

[20] Haq, E.U., Padmanabhan, S.K., & Licciulli, A. (2015). Microwave synthesis of thermal insulating foams from coal derived bottom ash. *Fuel Processing Technology*, 130, 263–267. [CrossRef]

[21] Dembovska, L., Bajare, D., Ducman, V., Korat, L., & Bumanis, G. (2017). The use of different by–products in the production of lightweight alkali activated building materials. *Construction and Building Materials*, 135, 315–322. [CrossRef]

[22] Akgül, E., & Tanaçan, L. (2011). Evaluation of the pozzolanic activity of the earth of Datça as a building material. *International Journal of Architectural Heritage*, 5, 1–26. [CrossRef]

[23] Ercan, T., Günay, E., Baş, H., & Can, B. (1984). Petrology of quaternary volcanic rocks in the Datca Peninsula and comment on their origin. *Bulletin of the Mineral Research and Exploration*, 97/98, 21–23. [Turkish]

[24] TS EN 196–6 (2010). Methods of testing cement – Part 6: Determination of fineness. *Turkish Standard Institution*, Ankara.

[25] T.S. 25 (2008). *Tras*. Turkish Standard Institution.

[26] Barış, K.E., & Tanaçan, L. (2021). Improving the geopolymeric reactivity of Earth of Datça as a Natural Pozzolan in developing green binder. *Journal of Building Engineering*, 41, Article 102760. [CrossRef]

[27] Hajimohammadi, A., Ngo, T., & Kashani, A. (2018). Glass waste versus sand as aggregates: The characteristics of the evolving geopolymer binders. *Journal of Cleaner Production*, 193, 593–603. [CrossRef]

[28] Wang, Y., Wang, Y., & Zhang, M. (2021). Effect of sand content on engineering properties of fly ash–slag based strain hardening geopolymer composites. *Journal of Building Engineering*, 34, Article 101951. [CrossRef]

[29] Jones, M.R., Ozlutas, K., & Zheng, L. (2015). Stability and instability of foamed concrete. *Magazine of Concrete Research*, 68(11), 1–8. [CrossRef]

[30] ASTM C1437–20 (2020). *Standard Test Method for Flow of Hydraulic Cement Mortar*. ASTM International, West Conshohocken.

[31] TS EN 1015–10 (2001). *Methods of test for mortar for masonry – Part 10: Determination of dry bulk density of hardened mortar*. Turkish Standard Institution, Ankara.

[32] TS EN 13755 (2009). *Natural stone test methods – Determination of water absorption at atmospheric pressure*. Turkish Standard Institution, Ankara.

[33] TS EN 14579 (2006). *Natural stone test methods – Determination of sound speed propagation*. Turkish Standard Institution, Ankara.

[34] TS EN 196–1 (2009). *Methods of testing cement – Part 1: Determination of strength*. Turkish Standard Institution, Ankara.

[35] ASTM C518–17 (2017). *Standard test method for steady–state thermal transmission properties by means of the heat flow meter apparatus*. ASTM International, West Conshohocken.

[36] Cui, Y., Wang, D., Zhao, J., Li, D., Ng, S., & Rui, Y. (2018). Effect of calcium stearate based foam stabilizer on pore characteristics and thermal conductivity of geopolymer foam material. *Journal of Building Engineering*, 20, 21–29. [CrossRef]

[37] Zhang, Z., Provis, J.L., Reid, A., & Wang, H. (2014). Geopolymer foam concrete: An emerging material for sustainable construction. *Construction and Building Materials*, 56, 113–127. [CrossRef]

[38] Gualtieri, M.L., Cavallini, A., & Romagnoli, M. (2016). Interactive powder mixture concept for the preparation of geopolymers with fine porosity. *Journal of European Ceramic Society*, 36(10), 2641–2646. [CrossRef]

[39] Kamseu, E., Ngouloure, Z.N.M., Ali, B.N., Zekeng, S., & Melo, U.C., Rossignol, S., Leonelli, C. (2015). Cumulative pore volume, pore size distribution and phases percolation in porous inorganic polymer composites: Relation microstructure and effective thermal conductivity. *Energy and Buildings*, 88, 45–56. [CrossRef]

[40] Lim, M.K., & Cao, H. (2013). Combining multiple NDT methods to improve testing effectiveness. *Construction and Building Materials*, 38, 1310–1315. [CrossRef]

[41] Hajimohammadi, A., Ngo, T., Mendis, P., Kashani, A., & van Deventer, J.S.J. (2017). Alkali activated slag foams: The effect of the alkali reaction on foam characteristics. *Journal of Cleaner Production*, 147, 330–339. [CrossRef]

[42] Hamad, A.J. (2014). Materials, production, properties and application of aerated lightweight concrete: Review. *International Journal of Materials Science and Engineering*, 2(2), 152–157. [CrossRef]

[43] Huang, Y., Gong, L., Shi, L., Cao, W., Pan, Y., & Cheng, X. (2018). Experimental investigation on the influencing factors of preparing porous fly ash–based geopolymer for insulation material. *Energy and Buildings*, 168, 9–18. [CrossRef]

[44] Zhang, Z., Provis, J.L., Reid, A., & Wang, H. (2015). Mechanical, thermal insulation, thermal resistance and acoustic absorption properties of geopolymer foam concrete. *Cement and Concrete Composites*, 62, 97–105. [CrossRef]

[45] Xu, F., Gu, G., Zhang, W., Wang, H., Huang, X., & Zhu, J. (2018). Pore structure analysis and properties evaluations of fly ash–based geopolymer foams by chemical foaming method. *Ceramics International*, 44(16), 19989–19997. [CrossRef]

[46] Zhang, Z., & Wang, H. (2016). The pore characteristics of geopolymer foam concrete and their impact on the compressive strength and modulus. *Frontiers in Materials*, 3, Article 38. [CrossRef]

[47] Prud'homme, E., Joussein, E., & Rossignol, S. (2015). Alkali–activated concrete binders as inorganic thermal insulator materials, Chapter 26, In: Pacheco–Torgal F, Labrincha JA, Leonelli C, Palomo A, Chindaprasirt P (Ed,). *Handbook of Alkali Activated Cements, Mortars and Concretes*, Woodhead Publishing, U.K., 687–728. [CrossRef]

[48] Gürdal, E. (1998). Isı iletkenlik katsayısının malzeme özellikleri ile ilişkileri. *Yapı*, 80, 44–46. [Turkish]

[49] Schlegel, E., Häussler, K., Seifert, H., & Freiberg, K. (1999). Microporosity and its use in highly efficient thermal insulating materials. *Cfi–Ceramic Forum International*, 76, 7–10.

[50] Dondi, M., Mazzanti, F., Principi, P., Raimondo, M., & Zanarini, G. (2004). Thermal conductivity of clay bricks. *Journal of Materials in Civil Engineering*, 16, 8–14. [CrossRef]

[51] Hajimohammadi, A., Ngo, T., & Kashani, A. (2018). Sustainable one–part geopolymer foams with glass fines versus sand as aggregates. *Construction and Building Materials*, 171, 223–231. [CrossRef]

[52] TS 825 (2013). Thermal insulation requirements for buildings. *Turkish Standard Institution*, Ankara.

[53] Haq, E.U., Padmanabhan, S.K., Zubair, M., Ali, L., & Licciulli, A. (2016). Intumescence behaviour of bottom ash based geopolymer mortar through microwave irradiation – As affected by alkali activation. *Construction and Building Materials*, 126, 951–956. [CrossRef]

[54] Novais, R.M., Ascensão, G., Buruberri, L.H., Senff, L., & Labrincha, J.A. (2016b). Influence of blowing agent on the fresh and hardened–state properties of lightweight geopolymers. *Materials Design*, 108, 551–559. [CrossRef]

[55] Palmero, P., Formia, A., Antonaci, P., Brini, S., & Tulliani, J.M. (2015). Geopolymer technology for application–oriented dense and lightened materials. Elaboration and characterization. *Ceramics International*, 41(10), 12967–12979. [CrossRef]

[56] Henon, J., Pennec, F., Alzina, A., Absi, J., Smith, D.S., & Rossignol, S. (2014). Analytical and numerical identification of the skeleton thermal conductivity of a geopolymer foam using a multi–scale analysis. *Computational Materials Science*, 82, 264–273. [CrossRef]

Dergi Kurulları

Honorary Editorial Advisory Board

Tarun Naik, professor emeritus, civil and environmental engineering, passed away on Jan. 29, 2024 (R.I.P).

Prof. Dr. Tarun R NAIK
UNİVERSİTY OF WİSCONSİN-MİLWAUKEE

İnşaat Mühendisliği, Betonarme Yapılar

Editor in Chief



Prof. Dr. Orhan CANPOLAT
YILDIZ TECHNICAL UNIVERSITY, FACULTY OF CIVIL ENGINEERING, DEPARTMENT OF CIVIL ENGINEERING
0000-0003-2744-7876
Türkiye Web
http://avesis.yildiz.edu.tr/canpolat/

Yapı Malzemeleri

Co-Editors

Prof. Dr. Rakesh KUMAR
CENTRAL ROAD RESEARCH INSTİTUTE
0000-0002-6723-4894
Hindistan

Yapı Malzemeleri

Prof. Dr. Benchaa BENABED
UNİVERSİTY OF LAGHOUAT DEPARTMENT OF CİVİL ENGİNEERİNG FACULTY OF CİVİL ENGİNEERİNG & ARCHİTECTURE, ALGERİA
Cezayir

İnşaat Mühendisliği, Yapı Malzemeleri

Dergi Kurulları



Prof. Dr. Messaoud SAIDANI
COVENTRY UNİVERSİTY
0000-0002-5861-676X

- Dergi Ana Sayfası
- Hakkında
- Amaç ve Kapsam
- Makale Gönder
- Dergi Kurulları
- İstatistikler
- Yazım Kuralları
- Etik İlkeler ve Yayın Politikası
- Ücret Politikası
- Dizinler
- Arşiv
- İletişim
- Author Contribution Form
- For Editors
- For Reviewers
- Copyright Form
- Archiving Policy
- Open Access



Birleşik Krallık

Betonarme Yapılar, Çelik Yapılar, Deprem Mühendisliği

Dr. Xiaojian GAO
SCHOOL OF CİVİL ENGİNEERİNG HARBİN INSTİTUTE OF TECHNOLOGY

Çin

İnşaat Mühendisliği, Betonarme Yapılar, Yapı Malzemeleri

Prof. Dr. Muammer KOÇ
HAMAD BİN KHALİFA UNİVERSİTY (HBKU) COLLEGE OF SCİENCE AND ENGİNEERİNG

Katar

Enerji Üretimi, Dönüşüm ve Depolama (Kimyasal ve Elektiksel hariç), Nanoteknoloji

Prof. Dr. Mustafa ŞAHMARAN
HACETTEPE UNİVERSİTY

Türkiye

Yapı Malzemeleri



Yrd. Doç. Dr. Sudharshan N. RAMAN
MONASH UNİVERSİTY MALAYSİA

0000-0003-4149-0141

Malezya Web

İnşaat Mühendisliği, Betonarme Yapılar, Mühendislik Tasarımı

Dr. Roman RABENSEIFER
SLOVAK UNİVERSİTY OF TECHNOLOGY İN BRATİSLAVA

Slovakya

Yeşil Yapılar ve Çevreler, Enerji Sistemleri Mühendisliği

Shengwen TANG
WUHAN UNİVERSİTY

Çin

Hidromekanik, Kırılma Mekaniği



Prof. Dr. Manuel F. M. COSTA
CENTER OF PHYSİCS OF THE UNİVERSİTY OF MİNHO AND OF THE UNİVERSİTY OF PORTO

0000-0002-1554-8779

Portekiz Web

Fen Bilgisi Eğitimi, Klasik ve Fiziksel Optik, Betonarme Yapılar, Ulaştırma Mühendisliği

Dr. A.s.m. Abdul AWAL
DEPARTMENT OF STRUCTURE AND MATERİALS, FACULTY OF CİVİL ENGİNEERİNG OF THE. UNİVERSİTİ TEKNOLOGİ MALAYSİA (UTM)
Malezya

İnşaat Mühendisliği, Betonarme Yapılar, Malzeme Bilimi ve Teknolojileri, Kompozit ve Hibrit Malzemeler

Prof. Dr. Ghazi AL-KHATEEB
JORDAN UNİVERSİTY OF SCİENCE AND TECHNOLOGY
Ürdün

Ulaştırma Mühendisliği



Prof. Dr. Murat ATES
TEKIRDAG NAMIK KEMAL UNIVERSITY
0000-0002-1806-0330
Türkiye Web

Fiziksel Kimya, Elektrokimya, Korozyon



Doç. Mohammad Arif KAMAL
ALİGARH MUSLİM UNİVERSİTY
0000-0001-8302-8794
Hindistan

Mimari Tasarım, Fiziksel Çevre Kontrolü

Dr. Aravind Krishna SWAMY
DEPARTMENT OF CİVİL ENGİNEERİNG, INDİAN INSTİTUTE OF TECHNOLOGY DELHİ
Hindistan

Ulaştırma Mühendisliği

Dr. Mohammed Mosleh SALMAN
COLLEGE OF ENGİNEERİNG AL-MUSTANSİRYA UNİVERSİTY
Irak

İnşaat Mühendisliği, Betonarme Yapılar, Malzeme Bilimi ve Teknolojileri, Kompozit ve Hibrit Malzemeler

Dr. Ali Naji ATTIYAH
UNİVERSİTY OF KUFA

Türkiye

Betonarme Yapılar



Prof. Dr. Soofia Tahira ELIAS-OZKAN
MIDDLE EAST TECHNICAL UNIVERSITY
Türkiye

Mimari ve Tasarım



Dr. Siyu REN
SCHOOL OF ECONOMİCS, NANKAİ UNİVERSİTY
Çin

Çevre Ekonomisi, Enerji Sistemleri Mühendisliği



Doç. Dr. Sepanta NAİMİ
ALTINBAŞ ÜNİVERSİTESİ, MÜHENDİSLİK VE MİMARLIK FAKÜLTESİ, İNŞAAT MÜHENDİSLİĞİ BÖLÜMÜ
0000-0001-8641-7090
Türkiye

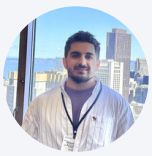
İnşaat Mühendisliği, Çelik Yapılar, Yapı Mühendisliği, Katı Mekanik



Yrd. Doç. Dr. Huachao YANG
ZHEJİANG UNİVERSİTY
Çin Web

Elektrik Enerjisi Üretimi (Yenilenebilir Kaynaklar Dahil, Fotovoltaikler Hariç), Jeotermal Enerji Sistemleri, Organik Yarı İletkenler, Nanoteknoloji

Proofreader Editor



Arş. Gör. Muhammed BAYRAM
TEXAS STATE UNİVERSİTY
0000-0001-6146-1394
Amerika Birleşik Devletleri

Yapı Malzemeleri, Yapı Mühendisliği

Language Editors

Geri Bildirim



Doktora Ömer Faruk KURANLI
YİLDİZ TECHNİCAL UNİVERSİTY
0000-0002-2937-1134
Türkiye

Mühendislik

Assistant Editor



Ekin PAYLAN
BİR KURUMA BAĞLI DEĞİLDİR
Türkiye

Journal of Sustainable Construction Materials and Technologies is open access journal under the CC BY-NC license (Creative Commons Attribution 4.0 International License)

Based on a work at https://dergipark.org.tr/en/pub/jscmt

E-mail: jscmt@yildiz.edu.tr

Dizinler

Her veri tabanından dergilerin dizin güncelliği kontrol edilmelidir. DergiPark sorumluluk almamaktadır.

Atıf Dizinleri

Scopus

TR Dizin

Diğer Dizinler

DOAJ

EBSCO Essentials

China National Knowledge Infrastructure (CNKI) Scholar

Sclit

- Dergi Ana Sayfası
- Hakkında
- Amaç ve Kapsam
- Makale Gönder
- Dergi Kurulları
- İstatistikler
- Yazım Kuralları
- Etik İlkeler ve Yayın Politikası
- Ücret Politikası
- Dizinler
- Arşiv
- İletişim
- Author Contribution Form
- For Editors
- For Reviewers
- Copyright Form
- Archiving Policy
- Open Access

Journal of Sustainable Construction Materials and Technologies is open access journal under the CC BY-NC license (Creative Commons Attribution 4.0 International License)

Based on a work at https://dergipark.org.tr/en/pub/jscmt

E-mail: jscmt@yildiz.edu.tr

Source details

Feedback > Compare sources >

Journal of Sustainable Construction Materials and Technologies

Open Access

Years currently covered by Scopus: from 2019 to 2024

Publisher: Kare Publishing

E-ISSN: 2458-973X

Subject area: Engineering: Building and Construction | Engineering: Civil and Structural Engineering | Energy: Renewable Energy, Sustainability and the Environment | Energy: General Energy

Source type: Journal

View all documents > | Set document alert | Save to source list

CiteScore 2023
0.8

SJR 2023
0.209

SNIP 2023
0.297

CiteScore | CiteScore rank & trend | Scopus content coverage

CiteScore 2023

$$0.8 = \frac{76 \text{ Citations } 2020 - 2023}{94 \text{ Documents } 2020 - 2023}$$

Calculated on 05 May, 2024

CiteScoreTracker 2024

$$1.6 = \frac{187 \text{ Citations to date}}{120 \text{ Documents to date}}$$

Last updated on 05 March, 2025 • Updated monthly

TR DİZİN

Giriş Yap

Yayın | Dergi | Yazar | Kurum

Journal of Sustainable Construction Materials and Technologies

ÜAK Doçentlik başvurularında yer alan "Ulusal Hakemli Dergi" tanımında yer alan ULAKBİM TR Dizin dergi listesidir.

Bulunan Toplam Sonuç : 1

Dergi Önerisi | Başlık A-Z

Filtrelerde Ara..

Yıl (4)

- 2024 1
- 2023 1
- 2022 1
- 2021 1

Yayın Dili (1)

- İngilizce 1

Konu (24)

Fen
- Mühendislik
- Temel Bilimler



Journal of sustainable construction materials and technologies (Online)

EISSN: 2458-973X

Editör Orhan Canpolat

2024 2023 2022 2021 **Web Adresi**

Toplam Kayıt: 1

ISSN 2458-973X

JSCMT

Journal of Sustainable Construction Materials and Technologies

Volume 7
Issue 3
Year 2022

YTU PRESS

www.jscmt.yildiz.edu.tr

Journal of Sustainable Construction Materials and Technologies

Volume: 7 Issue: 3, 9/30/22

YEAR: 2022

Research Articles

Research Article

1. Performance of dredged sediments based controlled low-strength material

Pranshoo Solanki *

Page : 119-127 PDF

Research Article

2. Natural pozzolan-based green geopolymer foam for thermal insulation

Kübra Ekiz Barış *, Leyla Tanaçan

Page : 128-144 PDF

Research Article

3. Characterization of carbon fiber reinforced conductive mortars filled with recycled ferrochrome slag aggregates

Fatih Doğan , Heydar Dehghanpour *, Serkan Subaşı , Muhammed Maraşlı

Page : 145-157 PDF

Research Article

4. Effect of Fiber Type, Shape and Volume Fraction on Mechanical and Flexural Properties of Concrete

Mahmut Başsürücü , Cenk Fenerli , Ceren Kına *, Şadiye Defne Akbaş

Page : 158-171 PDF

Research Article

5. An Evaluation of Vertical Dynamic Stress Attenuation for Compacted Coarse-Grained Soils

Kuangbiao Sun , Mingjing Fang *, Donglin Shu , Yang Pu , Wenbing Wang

Page : 172-183 PDF

Research Article



Download Cover Image

- ISSUE FILES
  - Tam Sayı

2.8K 7.4K 1

- Archive
  - Volume: 7 Issue: 1, 3/31/22
  - Volume: 7 Issue: 2, 6/28/22
  - Volume: 7 Issue: 3, 9/30/22
  - Volume: 7 Issue: 4, 12/30/22
  - Volume: 8 Issue: 1, 3/31/23

6. Assessment of the adoption of 3D printing technology for construction delivery: A case study of Lagos State, Nigeria

Akintayo Opawole *, Betty Oluwafunso Olojede , Kahilu Kajimo-shakantu

Page : 184-197 PDF

Review

7. Bibliographic analysis on 3D printing in the building and construction industry: Printing systems, material properties, challenges, and future trends

Qamar Shahzad *, Muhammad Umair , Saad Waqar

Page : 198-220 PDF

Review

8. Effect of Thermal Variances on Flexible Pavements

Michael Toryila Tiza *, Kavnen Jırgba , Habibu Abubakar Sanı , Terlumun Sesugh

Page : 220-230 PDF

Review

9. A review on engineering biocomposites and natural fiber-reinforced materials

Ataberk Baysal , Paşa Yayla *, Halit Süleyman Türkmen

Page : 231-249 PDF

Aim & Scope +

Writing Rules +

Ethical Principles and Publication Policy +

Price Policy +

Journal of Sustainable Construction Materials and Technologies is open access journal under the CC BY-NC license (Creative Commons Attribution 4.0 International License)

Based on a work at https://dergipark.org.tr/en/pub/jscmt

E-mail: jscmt@yildiz.edu.tr